ACS Combinatorial Science

Research Article

pubs.acs.org/acscombsci

Fluorescent Dye Cocktail for Multiplex Drug-Site Mapping on Human Serum Albumin

Jun Cheng Er,[†,‡] Marc Vendrell,[§] Mui Kee Tang,[†] Duanting Zhai,[†] and Young-Tae Chang*[,†,‡,∥]

[†]Department of Chemistry, National University of Singapore, 3 Science Drive 2, 117543 Singapore

[‡]Graduate School for Integrative Sciences and Engineering, National University of Singapore, Centre for Life Sciences, #05-01, 28 Medical Drive, 117456 Singapore

[§]MRC Centre for Inflammation Research, Queen's Medical Research Institute, University of Edinburgh, Edinburgh EH16 4TJ, United Kingdom

[∥]Laboratory of Bioimaging Probe Development, Singapore Bioimaging Consortium, Agency for Science, Technology and Research (A*STAR), 11 Biopolis Way, 138667 Singapore

S *Supporting Information*

ABSTRACT: Elucidating how molecules bind to HSA is fundamental for predicting drug incompatibilities. Through combinatorial screening, we identified a novel fluorescent dye (**BD140**) with turn-on fluorescence emission and specific binding at HSA drug site 2. We further combined it with dansylamide to develop a fluorescent dye cocktail for high-throughput mapping of the interaction between therapeutics at HSA drug-binding sites.

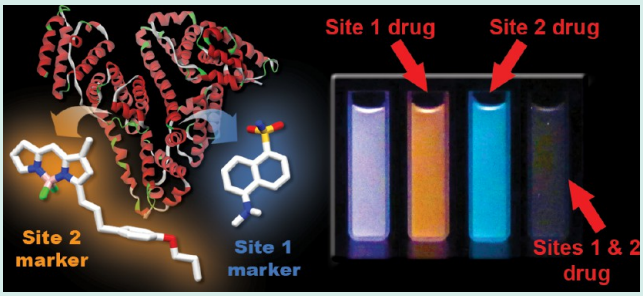

KEYWORDS: *drug discovery, fluorescence, high-throughput screening, human serum albumin, multiplex assays, pharmacokinetics*

INTRODUCTION

Human serum albumin (HSA), with a concentration of 0.6 mM in blood plasma, is an essential transporter protein for many drugs and endogenous compounds.[1,2] The study of HSA-drug interactions is of paramount importance, since the binding of drugs to albumin determines their pharmacokinetics, biodistribution and toxicity.[3−8] Crystallographic studies identified several binding pockets on HSA.[5,6,9−12] Among them, two sites (i.e., sites 1 and 2) located in the subdomains IIA and IIIA, have been identified as its primary drug binding sites.[13] The characterization of the binding of therapeutics at these sites is a critical step in predicting potential drug interactions. Crystallographic analysis,[14] radiolabeled probes,[15] and ^{19}F-labeled site specific ligands[16,17] cannot be applied to large collections of compounds. Alternatively, since the first site-specific HSA fluorescent probes[18] reported by Sudlow et al.,[19,20] a number of fluorescence assays have been developed.[21,22] However, due to the employment of dansyl ligands (e.g., dansylsarcosine, dansyl-L-norvaline and dansylamide)[19−21,23] or dyes that emit at similarly short wavelengths, only one binding site can be monitored in a single assay.[22,24] Herein, we report the first multiplex assay for the simultaneous analysis of drug interactions at the main HSA binding sites. Our assay is based on the combinatorial discovery of a site 2-specific fluorescent probe (**BD140**), whose emission does not overlap with dansyl fluorophores. We combined **BD140** and dansylamide (**DNSA**), a site 1-specific fluorescent probe, and developed a simple, high-throughput methodology for the examination of large collections of therapeutic drugs at HSA binding sites.

RESULTS AND DISCUSSION

We first amassed a collection of 3000 compounds from diversity-oriented combinatorial fluorescent libraries showing minimal emission overlap with dansyl fluorophores.[25−31] We analyzed their fluorescence response toward HSA and identified 20 compounds with significant fluorescence increase upon interaction with the protein. These primary hits were further examined for site-specificity using competition assays with warfarin and ibuprofen, which bind to HSA drug sites 1 and 2 respectively (see Figure S1 in the Supporting Information). **BD140** was selected for further development because of its high sensitivity (41-fold fluorescence quantum yield increase) and site 2-specificity (Figure 1).

BD140 showed a remarkable fluorescence emission upon binding to site 2 (Figure 2). We performed a Job plot to confirm the stoichiometry of the **BD140**:HSA complex. The fluorescence response peaked at 1:1 proportion, which confirms that **BD140** binds only at drug site 2 (see Figure S2 in the Supporting Information).[32,33] A one-site binding model was fitted to the titration of HSA to determine the dissociation

Received: April 28, 2013
Revised: June 23, 2013
Published: August 14, 2013

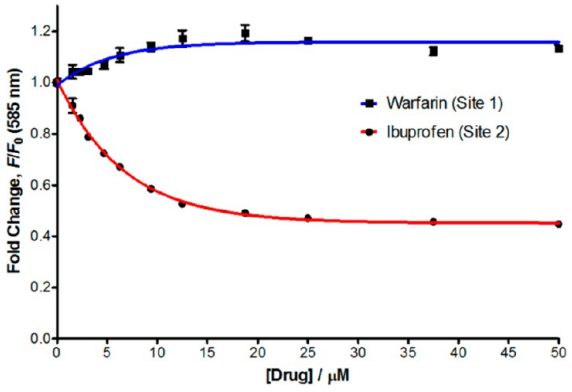

Figure 1. Competition of **BD140** with site-selective HSA-binding drugs. HSA (10 μM), **BD140** (3 μM), and the respective drugs (up to 50 μM) in 10 mM phosphate buffer (1% DMSO, pH 7.3) were incubated for 30 min. F is the fluorescence intensity at the indicated drug concentration, and F_0 is the fluorescence intensity with no drug added. λ_{exc} = 520 nm; λ_{em} = 585 nm. Values are represented as means and error bars as standard deviations (n = 3).

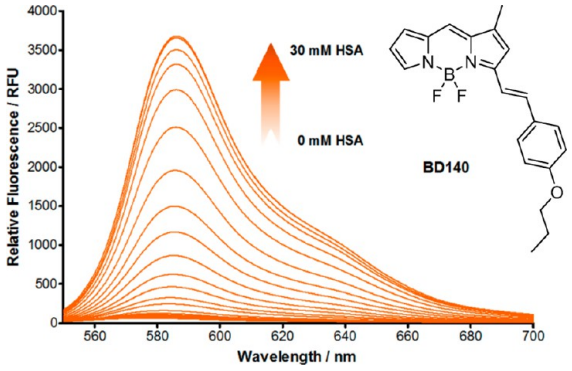

Figure 2. Emission spectra of **BD140** (3 μM) without HSA and upon incubation with serial dilutions of HSA (from 1.8 nM to 30 μM) in 10 mM phosphate buffer (1% DMSO, pH 7.3). λ_{exc} = 365 nm. Φ_F (without HSA) = 0.0035, Φ_F (in 30 μM HSA) = 0.15. Values are represented as means (n = 3).

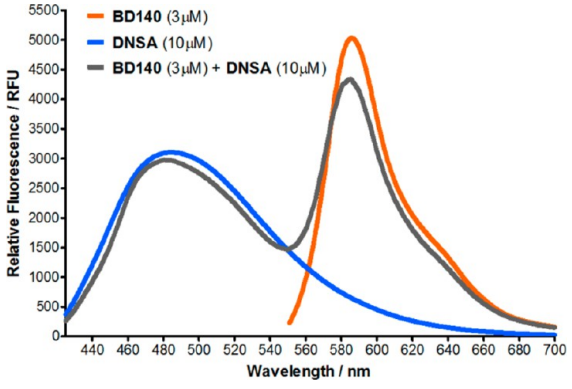

Figure 3. Emission spectrum of **BD140** (3 μM) and **DNSA** (10 μM) dye cocktail after incubation with HSA (10 μM) in 10 mM phosphate buffer (1% DMSO, pH 7.3) (*gray*). The spectrum of the mixture overlaps with the individual emission spectra of **BD140** (*orange*) and **DNSA** (*blue*). λ_{exc} = 365 nm. Values are represented as means (n = 3).

constant (K_D) of **BD140** as 4.1 ± 0.1 μM (see Figure S3 in the Supporting Information). After identifying a fluorescent turn-on probe with specific binding at site 2, we designed a multiplex assay for mapping HSA drug sites 1 and 2 using our **BD140**

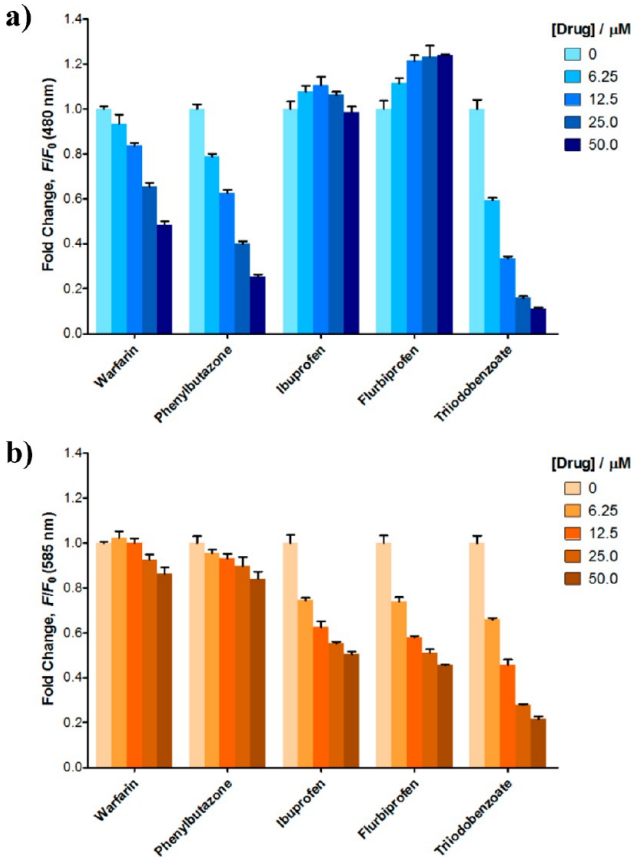

Figure 4. Analysis of HSA-binding drugs using multiplex fluorescent probes. HSA (10 μM), **BD140** (3 μM), **DNSA** (10 μM) and the respective drugs in 4 serial dilutions (10 mM phosphate buffer (1% DMSO, pH 7.3)) were incubated for 30 min. F is the fluorescence intensity with the drug added and F_0 is the fluorescence intensity with no drug added. λ_{exc} = 365 nm. (a) λ_{em} = 480 nm (site 1). (b) λ_{em} = 585 nm (site 2). Values are represented as means and error bars as standard deviations (n = 3).

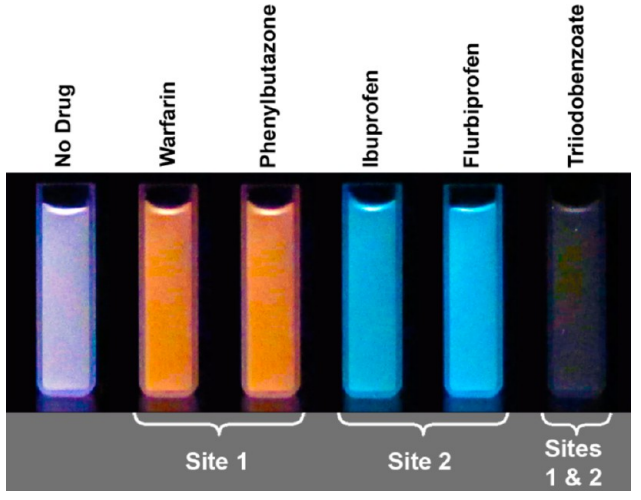

Figure 5. Fluorescence mapping of drugs binding sites on HSA. Solutions of **BD140** (3 μM), **DNSA** (10 μM), HSA (10 μM), and drugs (50 μM) in 10 mM phosphate buffer (1% DMSO, pH 7.3) were illuminated with a UV-lamp at 365 nm.

and **DNSA**, a commercially available site 1 probe.[19] We optimized the sensitivity of both probes using a 3:1 **DNSA**:**BD140** ratio and an excitation wavelength at 365 nm.

dx.doi.org/10.1021/co400060b | *ACS Comb. Sci.* 2013, 15, 452−457

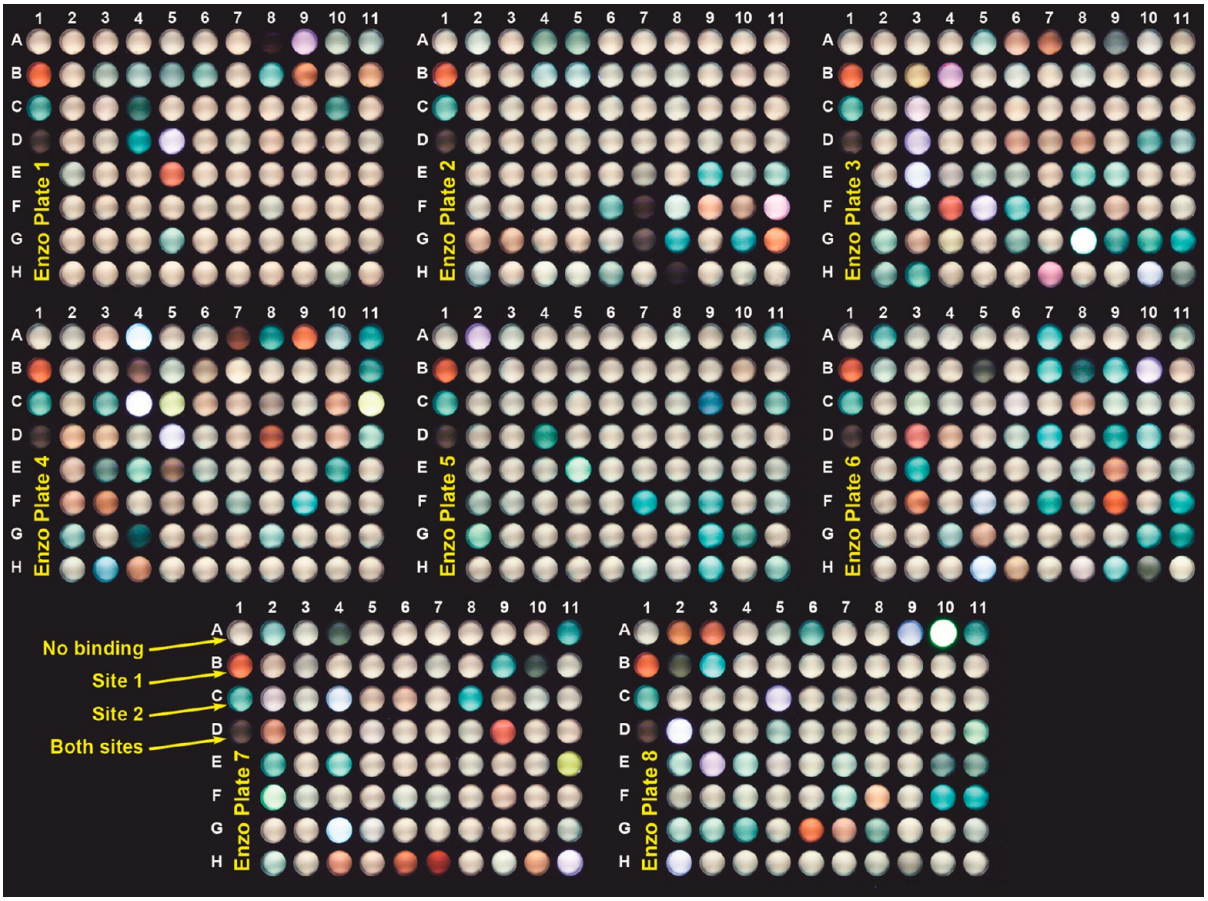

Figure 6. High-throughput mapping of HSA binding sites for 640 FDA-approved drugs. Solutions of **BD140** (3 μM), **DNSA** (10 μM), HSA (10 μM) and Enzo compounds (50 μM) in 10 mM phosphate buffer (2% DMSO, pH 7.3) were irradiated with a UV-lamp at 365 nm. For each plate: A1, no drug; B1, warfarin (site 1); C1, ibuprofen (site 2); D1, triiodobenzoate (sites 1 and 2); A2-H11, Enzo Screen-Well FDA Approved Drug Library. For the full list of compounds and their plate positions, see Table S1 in the Supporting Information. Drugs showing color change (orange (site 1), pale blue (site 2), or black (both sites)) are summarized in Table 1.

Under these conditions, the fluorescence emission intensity of both probes was comparable, which corroborated the multiplex capabilities of **BD140** with blue-emitting probes under one single excitation wavelength (Figure 3). Notably, the emission spectrum of the dye cocktail perfectly matched their separate spectra, which indicates their independent binding and confirmed that **DNSA** and **BD140** can be combined for the simultaneous mapping of drug sites 1 and 2.

To validate our multiplex system for mapping HSA drug sites, we examined 5 different HSA-binding drugs, namely warfarin, phenylbutazone, ibuprofen, flurbiprofen and triiodobenzoate. As illustrated in Figure 4, ibuprofen induced a dose-dependent decrease of **BD140** ($\lambda_{em(max)}$ = 585 nm) only, whereas warfarin decreased only the fluorescence emission of **DNSA** ($\lambda_{em(max)}$ = 480 nm). Triiodobenzoate, a drug binding to both sites 1 and 2, led to a fluorescence decrease in the entire emission range due to displacement of both dyes. Similarly, phenylbutazone and flurbiprofen elicited dose-dependent fluorescence responses consistent with their reported binding sites (i.e., phenylbutazone and flurbiprofen binds to site 1 and site 2 respectively).[5,13,16,19,34] Flurbiprofen induced a slight fluorescence increase in **DNSA** (Figure 4a), a phenomenon previously described by Sudlow et al. as due to increases in quantum yield of **DNSA** without significant changes in the amount of the bound probe.[20]

In view of the high sensitivity of our multiplex system, we evaluated whether a digital photograph of the fluorescent cocktail could provide a qualitative mapping of the binding at HSA. As shown in Figure 5, the irradiation of both dyes at 365 nm in the absence of HSA-binding drugs led to their respective blue and orange emission, which resulted in an overall white color. Displacement of **BD140** by the site 2 selective drugs, ibuprofen and flurbiprofen, selectively quenched the orange emission leaving only the blue fluorescence of **DNSA**. Likewise, site 1 selective drugs, warfarin and phenylbutazone, decreased the emission of **DNSA** and retained only the orange fluorescence of **BD140**. Triiodobenzoate, which displaced both dyes, removed all traces of fluorescence emission. These results indicate that our multiplex fluorescent probes can provide a qualitative readout of the binding sites of drugs without the need of a spectrophotometer, an essential feature for rapid and simple high-throughput screenings.

To validate the potential of our methodology for the high-throughput analysis of drug interactions at HSA, we screened the Enzo Screen-Well compound library, which consists of 640 U.S. Food and Drug Administration (FDA)-approved drugs. The drugs were distributed on eight 96-well plates, then HSA and the dye cocktail were added to each well, and the mixtures were incubated for 30 min before a digital photograph was taken under irradiation at 365 nm (Figure 6). From this simple readout, we could determine the compounds' binding

dx.doi.org/10.1021/co400060b | ACS Comb. Sci. 2013, 15, 452−457

Table 1. Therapeutic Drugs Classified by Their HSA Binding Sites

plate position[a]	drug
strong site 1	
1-B9	tolbutamide
1-B11	glipizide
1-E5	iodipamide
2-F10	nisoldipine
2-G11	candesartan
3-D6	nifedipine
3-D8	nitrendipine
3-F4	tranilast
4-A9	meloxicam
4-F3	glyburide
4-H4	fosinopril
6-E9	flutamide
6-F3	furosemide
6-F9	glimepiride
7-D2	pantoprazole
7-D9	phenylbutazone
7-E11	pyrantel pamoate
7-H4	sulfadoxine
7-H10	tenoxicam
8-A2	tetracycline
8-A3	tenatoprazole
8-G6	aprepitant
8-G7	bosentan
8-H9	L-thyroxine
strong site 2	
1-B4	amiodarone·HCL
1-B5	nicardipine·HCl
1-B6	pimozide
1-B8	fluspirilene
1-C10	rosiglitazone maleate
1-D4	naftopidil·2HCl
2-A4	furafylline
2-A5	nateglinide
2-E9	ticlopidine
2-F6	manidipine
2-G8	sertaconazole
2-G10	aripiprazole
3-D3	amiloride
3-D10	niguldipine
3-D11	flunarizine·2HCl
3-F6	bromocriptine
3-G6	capsaicin
3-G9	ethacrynic acid
3-G10	indomethacin
3-G11	naproxen
3-H3	ibuprofen
3-H11	docebenone
4-A8	(±)-ketoprofen
4-A10	terbinafine
4-A11	sodium phenylbutyrate
4-B11	troglitazone
4-C3	raloxifene
4-E10	fentiazac
4-F9	celecoxib
4-H3	fluvastatin
5-A11	lomerizine
5-C9	salmeterol

plate position[a]	drug
strong site 2	
5-D4	aceclofenac
5-F7	bifonazole
5-F9	bromhexine
5-G9	chlormadinone acetate
5-G10	chlorambucil
5-H9	clomiphene
6-A2	clobetasol propionate
6-A7	cyproterone acetate
6-B7	diethylstilbestrol
6-B9	disulfiram
6-D7	fenbufen
6-D9	fenoprofen
6-D10	fenofibrate
6-E3	flurbiprofen
6-F7	gemfibrozil
6-F11	hexestrol
6-G4	17-hydroxyprogesterone
6-G10	itraconazole
6-G11	(*S*)-(+)-ketoprofen
6-H9	loratadine
7-A11	miconazole
7-B9	nefazodone
7-C8	oxiconazole
7-E2	pranoprofen
8-A6	tioconazole
8-A11	toremifene
8-B3	tolmetin
8-F10	butoconazole nitrate
8-F11	mifepristone
8-G4	tamoxifen
8-G8	efavirenz
strong sites 1 and 2	
1-A8	lomofungin
1-C4	flufenamic acid
2-F7	tolcapone
2-G7	atovaquone
2-H8	entacapone
3-A7	aclarubicin
3-A9	fenretinide
4-A7	nimesulide
4-B4	idebenone
4-C8	mitomycin C
4-D8	pranlukast
4-E3	valproic acid
4-E5	zafirlukast
4-G4	anethole-trithione
6-B5	diclofenac
6-B8	diflunisal
6-D3	etretinate
6-H10	lorglumide
7-A4	mefenamic acid
7-B10	niflumic acid
7-H6	sulfadimethoxine
7-H7	sulfasalazine
8-B2	tolfenamic acid
8-E10	trequinsin·HCL
8-E11	vinpocetine

[a]Enzo plate number-(row)(column).

dx.doi.org/10.1021/co400060b | *ACS Comb. Sci.* 2013, 15, 452−457

sites and identified 112 drugs showing a clear displacement of **BD140**, **DNSA**, or both (Table 1). This is the first report of a systematic screening for HSA-binding drugs that can be used to identify potential incompatibilities between commonly used therapeutics. Drugs with comparable HSA binding may exhibit competition if they are coadministrated. For example, an increased bioavailability of nimesulide, a nonsteroidal anti-inflammatory drug (NSAID) binding at HSA drug sites 1 and 2, has been observed when used concurrently with tolbutamide (site 1) or fenofibrate (site 2).[35] Similarly, nicardipine, a site 2 binding antianginal drug, has been reported to increase the effects of nateglinide, nefazodone (site 2), zafirlukast and diclofenac (sites 1 and 2).[35] On the other hand, pantoprazole (site 1), a drug for treating gastresophageal reflux disease, increases levels of other site 1 drugs, such as glipizide, glimepiride, bosentan, and warfarin.[35] This multiplex assay provides essential information on drug interactions that may have been unknown to clinicians, and can rapidly elucidate the HSA binding sites of new molecular entities as well as obtain fundamental knowledge of their pharmacodynamic profile.

CONCLUSION

In summary, we identified a novel HSA drug site 2-specific fluorescent probe (**BD140**) and optimized a fluorescent dye cocktail to map major HSA drug binding sites. This methodology represents the first fluorescent multiplex assay to analyze the binding of therapeutics to HSA in a high-throughput manner and without the need of spectrophotometers. We proved the value of our methodology by examining a collection of 640 FDA-approved drugs and elucidating the HSA-binding sites of 112 common therapeutic drugs for the first time. This information is crucial to identify incompatibilities between drugs that are administrated together. The simplicity of our methodology makes it a valuable tool for high-throughput drug screening and rapid identification of drug interactions.

EXPERIMENTAL PROCEDURES

Materials. All commercially available reagents, solvents and proteins were purchased from Sigma Aldrich, Alfa Aesar, Fluka, Merck, or Acros, and used as received unless otherwise stated. Ibuprofen, warfarin, triiodobenzoic acid, flurbiprofen, and dansylamide were purchased from Sigma Aldrich. Phenylbutazone was purchased from Tokyo Chemical Industry Co., Ltd. Screen-Well FDA Approved Drug Library was purchased from Enzo Life Sciences.

Methods and Measurements. Spectroscopic and quantum yield data were measured on a SpectraMax M2 spectrophotometer (Molecular Devices). Data analysis was performed using GraphPrism 5.0. Mixtures of **BD140** and **DNSA** with HSA were prepared in phosphate buffer (1% DMSO, pH 7.3) at room temperature and fluorescence measurements were taken after incubation for 30 min unless otherwise stated. Analytical characterization was performed on a HPLC-MS (Agilent-1200 series) with a DAD detector and a single quadrupole mass spectrometer (6130 series) with an ESI probe. Analytical HPLC method: eluents, A: H_2O (0.1% HCOOH), B: CH_3CN (0.1% HCOOH), gradient 5% B to 95% B (10 min). Reverse-phase Phenomenex C_{18} Luna column (4.6 × 50 mm^2, 3.5 μm particle size), flow rate: 1 mL/min. ^1H NMR, ^{19}F-NMR, and ^{13}C NMR spectra were recorded on Bruker ACF300 (300 MHz) and AMX500 (500 MHz) spectrometers and reported in δ (ppm). ^1H NMR spectra were referenced to residual proton signals in CD_3CN (δ = 1.94 ppm); ^{13}C NMR spectra were referenced to solvent resonances of CD_3CN (δ = 1.32 ppm); ^{19}F NMR spectra were referenced to external TFA (δ = −76.55 ppm vs $CFCl_3$ at 0.00 ppm). High resolution mass spectra (ESI) were obtained on a Finnigan/MAT 95XL-T spectrometer. A UV lamp (Spectroline, XX-15NF/FB, 254/365 nm) was used to illuminate the HSA-dye-drug solutions for fluorescence observation.

Quantum Yield Calculations. Quantum yields of **BD140** (3 μM) in its respective aqueous environments were calculated by measuring the integrated emission area of the fluorescent spectra (λ_{exc} = 505 nm) and comparing to the area measured for Rhodamine B (3 μM, Φ_F = 0.31, λ_{exc} = 505 nm) in water:

$$\Phi_F^{\mathrm{BD140}} = \Phi_F^{\mathrm{Rhodamine\ B}}\left(\frac{F^{\mathrm{BD140}}}{F^{\mathrm{Rhodamine\ B}}}\right)$$

where F represents the area of fluorescent emission. Emission was integrated between 535 and 700 nm.

(*E*)-5,5-difluoro-9-methyl-7-(4-propoxystyryl)-5*H*-dipyrrolo[1,2-*c*:2′,1′-*f*][1,3,2]diazaborinin-4-ium-5-uide (BD140). 1,3-Dimethyl 4,4-Difluoro-4-bora-3*a*,4*a*-diaza-*s*-indacene (1,3-dimethyl-BODIPY) was synthesized following the procedure described in ref 1.[26] The BODIPY (20 mg, 91 μmol), 4-propoxybenzaldehyde (29.6 mg, 182 μmol, 2 equiv), pyrrolidine (45 μL, 0.55 mmol, 6 equiv), and acetic acid (32 μL, 0.55 mmol, 6 equiv) were dissolved in 2 mL of acetonitrile and heated at 85 °C until the reaction was completed (approximately 5 min). The solvent was evaporated in vacuo and the resulting residue purified by flash column chromatography on silica gel (hexane/EtOAc, 4:1) to afford **BD140** as a dark pink solid (20 mg, 56 μmol, 61% yield). ^1H NMR (500 MHz, CD_3CN): δ = 7.43 − 7.33 (m, 4H), 7.21 (s, 2H), 7.19 (d, J = 15.4 Hz, 2H), 6.78 (d, J = 3.3 Hz, 1H), 6.77−6.74 (m, 2H), 6.69 (s, 1H), 6.26 (dd, J = 3.7, 2.1 Hz, 1H), 3.78 (t, J = 6.6 Hz, 2H), 2.11 (s, 3H), 1.58 (qt, J = 7.4, 6.6 Hz, 2H), 0.81 (t, J = 7.4 Hz, 4H). ^{13}C NMR (125 MHz, CD_3CN): δ = 162.1, 160.8, 147.1, 142.1, 139.1, 138.3, 133.9, 130.6, 129.3, 126.3, 124.3, 116.2, 116.1, 70.6, 23.2, 11.6, 10.6. ^{19}F NMR (282 MHz, CD_3CN): δ = −139.82 to −145.59 (m). HRMS ($C_{21}H_{21}BF_2N_2O$): Calcd $[M + Na]^+$ 389.1613, Found $[M + Na]^+$ 389.1611.

ASSOCIATED CONTENT

Supporting Information

Selected fluorescent dye hits for HSA, additional binding studies of **BD140**; chemical structures, plate position and drug binding sites for Enzo Screen-Well FDA Approved Drug Library, and full characterization data (NMR, HR-MS) for **BD140.** This material is available free of charge via the Internet at http://pubs.acs.org.

AUTHOR INFORMATION

Corresponding Author

*Fax: +65 6779 1691. Tel: +65 6779 7794. E-mail: chmcyt@nus.edu.sg.

Author Contributions

The manuscript was written through contributions of all authors. All authors have given approval to the final version of the manuscript.

Funding

The authors acknowledge the financial support from a Singapore Ministry of Education Academic Research Fund Tier 2 (MOE2010-T2-2-030).

Notes

The authors declare no competing financial interest.

■ ACKNOWLEDGMENTS

E. J. C. thanks NGS for a scholarship. M.V. acknowledges the support of the Medical Research Council. The authors also thank Dr. Liyun Zhang (Hefei Institutes of Physical Science, Chinese Academy of Sciences) for her valuable discussion and advice.

■ ABBREVIATIONS

HSA, human serum albumin; DNSA, dansylamide; FDA, Food and Drug Administration; NSAID, nonsteroidal anti-inflammatory drug

■ REFERENCES

(1) Theodore Peters, J. *All About Albumin: Biochemistry, Genetics and Medical Applications*; Academic Press: San Diego, 1996.
(2) Fasano, M.; Curry, S.; Terreno, E.; Galliano, M.; Fanali, G.; Narciso, P.; Notari, S.; Ascenzi, P. The extraordinary ligand binding properties of human serum albumin. *IUBMB Life* **2005**, *57*, 787−796.
(3) Fanali, G.; di Masi, A.; Trezza, V.; Marino, M.; Fasano, M.; Ascenzi, P. Human serum albumin: From bench to bedside. *Mol. Aspects Med.* **2012**, *33*, 209−290.
(4) Kragh-Hansen, U. Structure and ligand binding properties of human serum albumin. *Dan. Med. Bull.* **1990**, *37*, 57−84.
(5) He, X. M.; Carter, D. C. Atomic structure and chemistry of human serum albumin. *Nature* **1992**, *358*, XI−215.
(6) Carter, D. C.; Ho, J. X. Structure of serum albumin. *Adv. Prot. Chem.* **1994**, *45*, 153−203.
(7) Kragh-Hansen, U. Molecular aspects of ligand binding to serum albumin. *Pharmacol. Rev.* **1981**, *33*, 17−53.
(8) Varshney, A.; Sen, P.; Ahmad, E.; Rehan, M.; Subbarao, N.; Khan, R. H. Ligand binding strategies of human serum albumin: How can the cargo be utilized? *Chirality* **2010**, *22*, 77−87.
(9) Curry, S.; Mandelkow, H.; Brick, P.; Franks, N. Crystal structure of human serum albumin complexed with fatty acid reveals an asymmetric distribution of binding sites. *Nat. Struct. Mol. Biol.* **1998**, *5*, 827−835.
(10) Curry, S.; Brick, P.; Franks, N. P. Fatty acid binding to human serum albumin: new insights from crystallographic studies. *Biochim. Biophys. Acta, Mol. Cell Biol. L.* **1999**, *1441*, 131−140.
(11) Yang, F.; Bian, C.; Zhu, L.; Zhao, G.; Huang, Z.; Huang, M. Effect of human serum albumin on drug metabolism: Structural evidence of esterase activity of human serum albumin. *J. Struct. Biol.* **2007**, *157*, 348−355.
(12) Zhu, L.; Yang, F.; Chen, L.; Meehan, E. J.; Huang, M. A new drug binding subsite on human serum albumin and drug−drug interaction studied by X-ray crystallography. *J. Struct. Biol.* **2008**, *162*, 40−49.
(13) Ghuman, J.; Zunszain, P. A.; Petitpas, I.; Bhattacharya, A. A.; Otagiri, M.; Curry, S. Structural basis of the drug-binding specificity of human serum albumin. *J. Mol. Biol.* **2005**, *353*, 38−52.
(14) Curry, S. Lessons from the crystallographic analysis of small molecule binding to human serum albumin. *Drug Metab. Pharmacokinet.* **2009**, *24*, 342−357.
(15) Sjöholm, I.; Ekman, B.; Kober, A.; Ljungstedt-Påhlman, I.; Seiving, B.; Sjödin, T. Binding of drugs to human serum albumin. *Mol. Pharmacol.* **1979**, *16*, 767−777.
(16) Jenkins, B. G.; Lauffer, R. B. Detection of site-specific binding and co-binding of ligands to human serum albumin using 19F NMR. *Mol. Pharmacol.* **1990**, *37*, 111−118.
(17) Jenkins, B. G. Detection of site-specific binding and co-binding of ligands to macromolecules using 19F NMR. *Life Sci.* **1991**, *48*, 1227−1240.
(18) Wright, A. T.; Griffin, M. J.; Zhong, Z.; McCleskey, S. C.; Anslyn, E. V.; McDevitt, J. T. Differential receptors create patterns that distinguish various proteins. *Angew. Chem., Int. Ed.* **2005**, *44*, 6375−6378.
(19) Sudlow, G.; Birkett, D. J.; Wade, D. N. The characterization of two specific drug binding sites on human serum albumin. *Mol. Pharmacol.* **1975**, *11*, 824−832.
(20) Sudlow, G.; Birkett, D. J.; Wade, D. N. Further characterization of specific drug binding sites on human serum albumin. *Mol. Pharmacol.* **1976**, *12*, 1052−1061.
(21) Epps, D. E.; Raub, T. J.; Kézdy, F. J. A general, wide-range spectrofluorometric method for measuring the site-specific affinities of drugs toward human serum albumin. *Anal. Biochem.* **1995**, *227*, 342−350.
(22) Min, J.; Lee, J. W.; Ahn, Y.-H.; Chang, Y.-T. Combinatorial dapoxyl dye library and its application to site selective probe for human serum albumin. *J. Comb. Chem.* **2007**, *9*, 1079−1083.
(23) Ryan, A. J.; Ghuman, J.; Zunszain, P. A.; Chung, C. W.; Curry, S. Structural basis of binding of fluorescent, site-specific dansylated amino acids to human serum albumin. *J. Struct. Biol.* **2011**, *174*, 84−91.
(24) Baldridge, A.; Feng, S.; Chang, Y.-T.; Tolbert, L. M. Recapture of GFP chromophore fluorescence in a protein host. *ACS Comb. Sci.* **2011**, *13*, 214−217.
(25) Ahn, Y.-H.; Lee, J.-S.; Chang, Y.-T. Combinatorial rosamine library and application to in vivo glutathione probe. *J. Am. Chem. Soc.* **2007**, *129*, 4510−4511.
(26) Lee, J. S.; Kang, N. Y.; Kim, Y. K.; Samanta, A.; Feng, S.; Kim, H. K.; Vendrell, M.; Park, J. H.; Chang, Y. T. Synthesis of a BODIPY library and its application to the development of live cell glucagon imaging probe. *J. Am. Chem. Soc.* **2009**, *131*, 10077−82.
(27) Zhai, D.; Lee, S.-C.; Vendrell, M.; Leong, L. P.; Chang, Y.-T. Synthesis of a novel BODIPY library and its application in the discovery of a fructose sensor. *ACS Comb. Sci.* **2012**, *14*, 81−84.
(28) Vendrell, M.; Krishna, G. G.; Ghosh, K. K.; Zhai, D.; Lee, J.-S.; Zhu, Q.; Yau, Y. H.; Shochat, S. G.; Kim, H.; Chung, J.; Chang, Y.-T. Solid-phase synthesis of BODIPY dyes and development of an immunoglobulin fluorescent sensor. *Chem. Commun.* **2011**, *47*, 8424.
(29) Samanta, A.; Vendrell, M.; Das, R.; Chang, Y.-T. Development of photostable near-infrared cyanine dyes. *Chem. Commun.* **2010**, *46*, 7406.
(30) Er, J. C.; Tang, M. K.; Chia, C. G.; Liew, H.; Vendrell, M.; Chang, Y.-T. MegaStokes BODIPY-triazoles as environmentally sensitive turn-on fluorescent dyes. *Chem. Sci.* **2013**, *4*, 2168−2176.
(31) Kang, N.-Y.; Lee, S.-C.; Park, S.-J.; Ha, H.-H.; Yun, S.-W.; Kostromina, E.; Gustavsson, N.; Ali, Y.; Chandran, Y.; Chun, H.-S.; Bae, M.; Ahn, J. H.; Han, W.; Radda, G. K.; Chang, Y.-T. Visualization and isolation of langerhans islets by a fluorescent probe PiY. *Angew. Chem., Int. Ed.* **2013**, *52*, 8557−8560.
(32) Job, P. Formation and stability of inorganic complexes in solution. *Ann. Chim. Anal.* **1928**, *9*, 113−203.
(33) Huang, C. Y. Determination of binding stoichiometry by the continuous variation method: The Job plot. *Meth. Enzymol.* **1982**, *87*, 509−525.
(34) Kober, A.; Sjoholm, I. The binding sites on human serum albumin for some nonsteroidal antiinflammatory drugs. *Mol. Pharmacol.* **1980**, *18*, 421−426.
(35) Yeo, B. In *Master Index of Medical Specialties*, 131st ed.; Fun, L. W., Fancisco, J. C., Pena, L. A. D., Tamolang, S. E. V., Mirano, M. T. B., Patriarca, A. C., Pingol, M. F. Q., Solivet, Z. J. N., Eds.; UBM Medica Asia Pte Ltd.: Singapore, 2012.